

Design, Synthesis, and Characterization of 1,3,5-Tri(1*H*-benzo[*d*]imidazol-2-yl)benzene-Based Fluorescent Supramolecular Columnar Liquid Crystals with a Broad Mesomorphic Range

Jin-Feng Xiong,^{†,⊥} Shi-He Luo,^{‡,⊥} Jing-Pei Huo,[§] Jin-Yan Liu,[†] Shui-Xia Chen,^{*,‡} and Zhao-Yang Wang^{*,†}

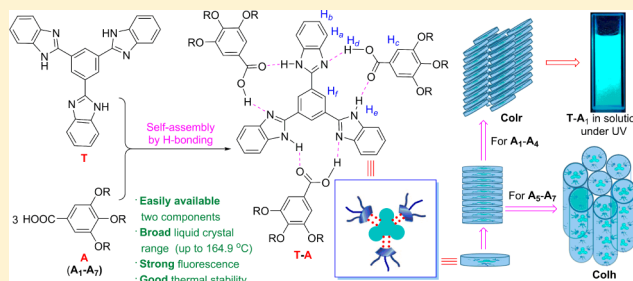
[†]School of Chemistry and Environment, South China Normal University, and Key Laboratory of Theoretical Chemistry of Environment, Ministry of Education, Guangzhou 510006, P. R. China

[‡]PCFM & DSAPM Lab, School of Chemistry and Chemical Engineering, Sun Yat-Sen University, Guangzhou 510275, China

[§]School of Chemistry and Chemical Engineering, South China University of Technology, Guangzhou 510640, P. R. China

Supporting Information

ABSTRACT: A new kind of supramolecular columnar liquid crystal **T–A** with a broad mesomorphic range (up to 164.9 °C), good thermal stability, and strong fluorescence is designed and formed by the H-bonding between 1,3,5-tri(1*H*-benzo[*d*]imidazol-2-yl)benzene (**T**) and serial gallic acid derivatives (**A**). Two components are easily available because of simple routes, common reactions, high yields, commercial starting materials, and inexpensive catalysts. The introduction of the 1,2,3-triazole structure into component **A** makes the textures different and is slightly disadvantageous for the **T–A** complexes.



1. INTRODUCTION

Self-assembly by H-bonding is an important method for forming liquid crystals, and liquid crystals based on H-bonding have many special advantages. In particular, they may exhibit dynamic behaviors, such as charge or energy transportation, information storing, and molecular sensing.^{1–3} At the same time, columnar liquid crystals with the function of transferring charge or energy are important photoelectric materials in many fields, including solar cells.^{4–6} Thus, there is an increasing level of interest in the study of columnar liquid crystals based on H-bonding. Usually, most columnar liquid crystals are formed by H-bonding in a one-component system.^{7–12}

To further apply H-bonding to multifunctional columnar liquid crystals, Sierra^{13–16} and other groups^{17–22} began to investigate the two-component system. In particular, if there is a fluorophore in one of the components, fluorescent columnar liquid crystals can be achieved as potential photoelectric materials.^{15,20} However, to the best of our knowledge, there are only two reports of fluorescent supramolecular columnar liquid crystals with a narrow liquid crystal phase based on H-bonding in a two-component system, and the fluorophores are introduced into the two-component system through lengthy synthetic routes.^{15,20} Thus, it is still a challenge to develop a new two-component system concisely and obtain liquid crystal materials with better properties.

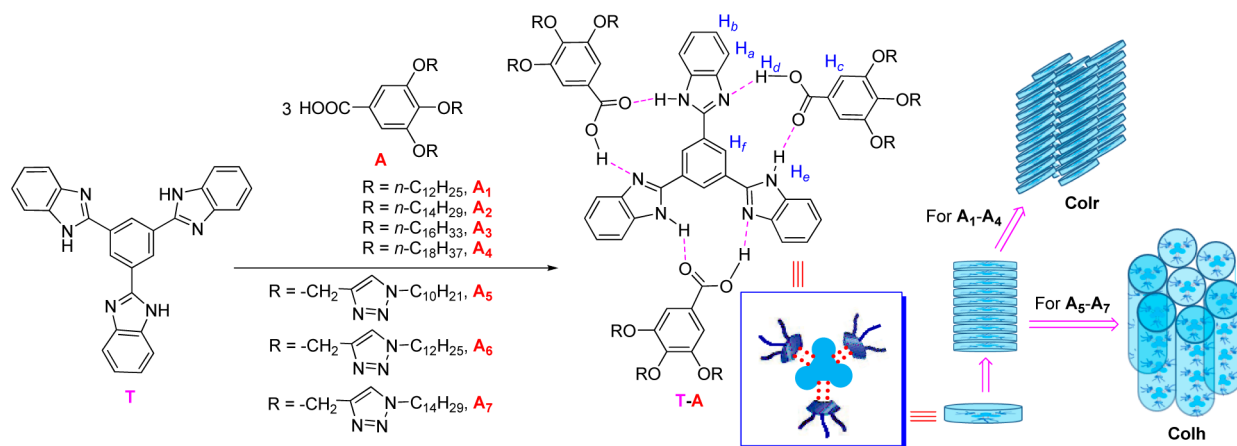
Herein, a new kind of fluorescent supramolecular columnar liquid crystals (**T–A**) with a broad mesomorphic range via H-

bonding between 1,3,5-tri(1*H*-benzo[*d*]imidazol-2-yl)benzene (**T**) and gallic acid derivatives (**A**) are reported (Scheme 1). Benzimidazole-type compound 1,3,5-tri(1*H*-benzo[*d*]imidazol-2-yl)benzene is designed as a component of liquid crystal materials for the first time, and two components are easily available because of simple routes, common reactions, high yields, commercial starting materials, and inexpensive catalysts (Schemes 2 and 3).

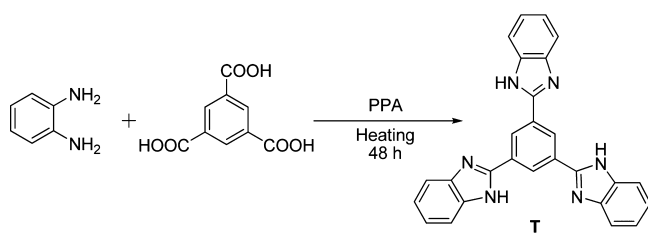
2. RESULTS AND DISCUSSION

2.1. Synthesis of Components T and A. Though 1,3,5-tri(1*H*-benzo[*d*]imidazol-2-yl)benzene is designed as component **T** for the first time (Scheme 1), this fluorescent core can be easily prepared by the simple condensation of commercially available *o*-phenylenediamine and trimesic acid (Scheme 2). Furthermore, the one-step reaction is catalyzed by inexpensive polyphosphoric acid, and the yield is 81%. In the literature about two-component fluorescent supramolecular columnar liquid crystals based on H-bonding, the synthesis of the fluorescent component has many shortcomings, such as the long synthetic route with a low total yield (the yield of three steps is 52–56%),¹⁵ and even five steps (the yield of the target molecule is 30–59%).²⁰ What is worse is the fact that the protection and deprotection steps are also needed,^{15,20} and

Received: July 28, 2014

Scheme 1. Formation of Supramolecular Columnar Liquid Crystals Based on 1,3,5-Tri(1*H*-benzo[*d*]imidazol-2-yl)benzene

Scheme 2. Synthetic Route of Component T



some steps require metal catalysis.²⁰ Therefore, it is obvious that, compared with the reported component,^{15,20} the fluorescent core T in our design can be concisely obtained with a higher yield in the absence of any metal catalyst.

At the same time, as component A, serial gallic acid derivatives [**A**₁–**A**₇ (Scheme 1)] are prepared in good yields through simple etherification, O-alkylation, Click reaction (for only **A**₅–**A**₇, which are designed to investigate the influence of the introduction of the 1,2,3-triazole structure into component A on the properties of the T–A complexes as a comparison because of the application of 1,2,3-triazole compounds in columnar liquid crystals^{20,23}), and hydrolysis reaction (Scheme 3), and the structures and purities of all T and A components are verified well by ¹H and ¹³C NMR, ESI-MS, FTIR, UV, and elemental analysis (see the Supporting Information).

2.2. Formation and Characterization of T–A Complexes. Using the reported methods,^{13,15,18,20} the T–A complexes are prepared, and their formation is studied via FTIR and NMR spectroscopy. Taking T–**A**₁ as an example

Scheme 3. Synthetic Route of Component A

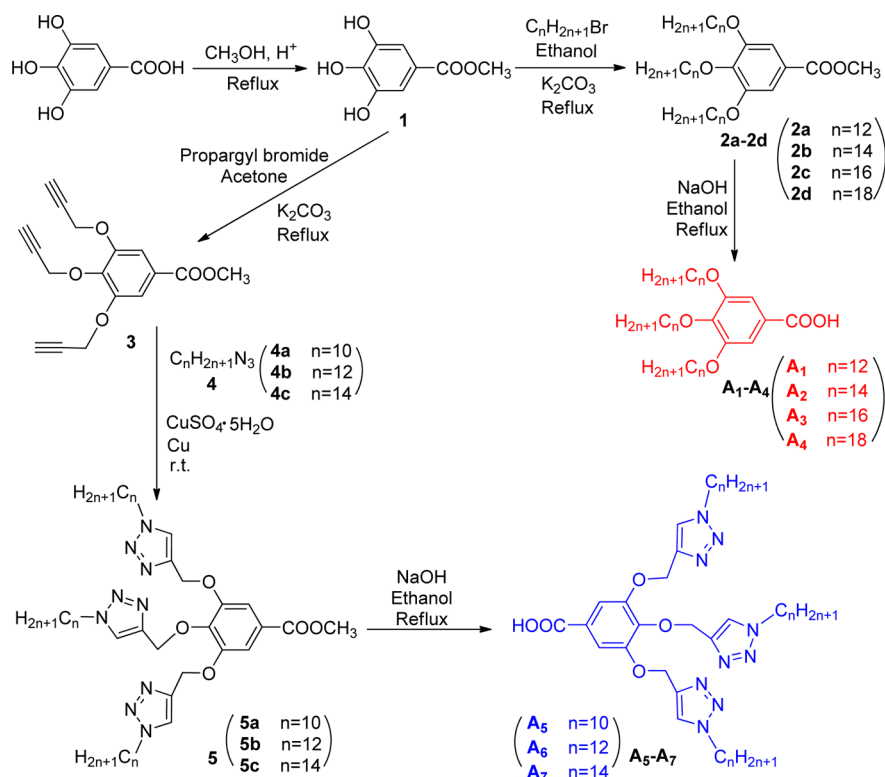


(Figure 1), the C=O stretching vibration in **A**₁ appears at 1683 cm⁻¹, which indicates dimeric H-bonding.²⁴ Conversely, the

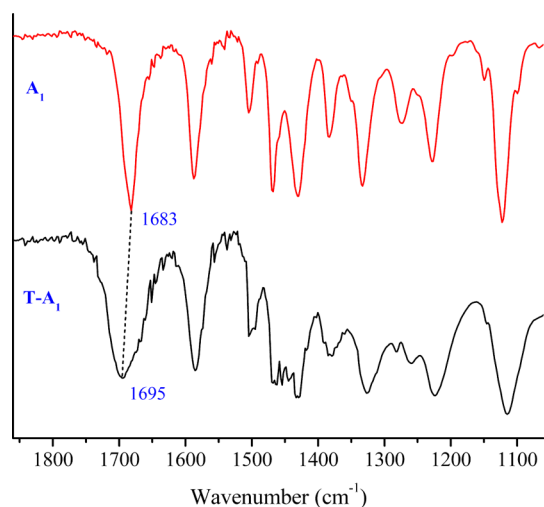


Figure 1. FTIR spectra of **A**₁ and **T-A**₁.

carbonyl band in **T-A**₁ is shifted to 1695 cm⁻¹, which is lower than that of the free carboxylic acid (1733 cm⁻¹). These results are similar to the corresponding results of the reported two-component columnar liquid crystal system.^{13,15,18,20}

Of course, the formation of H-bonding complexes as designed is further confirmed by the ¹H NMR investigation (Figure 2; more figures and detailed discussions can be seen in the Supporting Information). As anticipated, integral ratios of proton peaks are consistent with both the theoretical value and the molar feed ratios, and the proton signals involved in complexation as well as those near the complexing groups have field shifted in a correlated way (Figure 2), which is similar to the previously reported result.^{13,15,18,20}

2.3. Photophysical Properties and Thermal Stability.

According to the literature,^{20,25} the optical properties of the **T-A** complexes are investigated in dilute CH₂Cl₂ solutions (1 × 10⁻⁵ mol L⁻¹ for the UV-vis absorption measurement and 1 × 10⁻⁶ mol L⁻¹ for the fluorescence measurement) at room temperature. For the **T-A**₁ complex, there are two absorption peaks at 276 and 311 nm and an emission maximal wavelength (λ_{ex}) at 375 nm (Figure 3, left). When the 1,2,3-triazole structure is introduced into component **A**, there is a similar curve (Figure S3 of the Supporting Information), while the

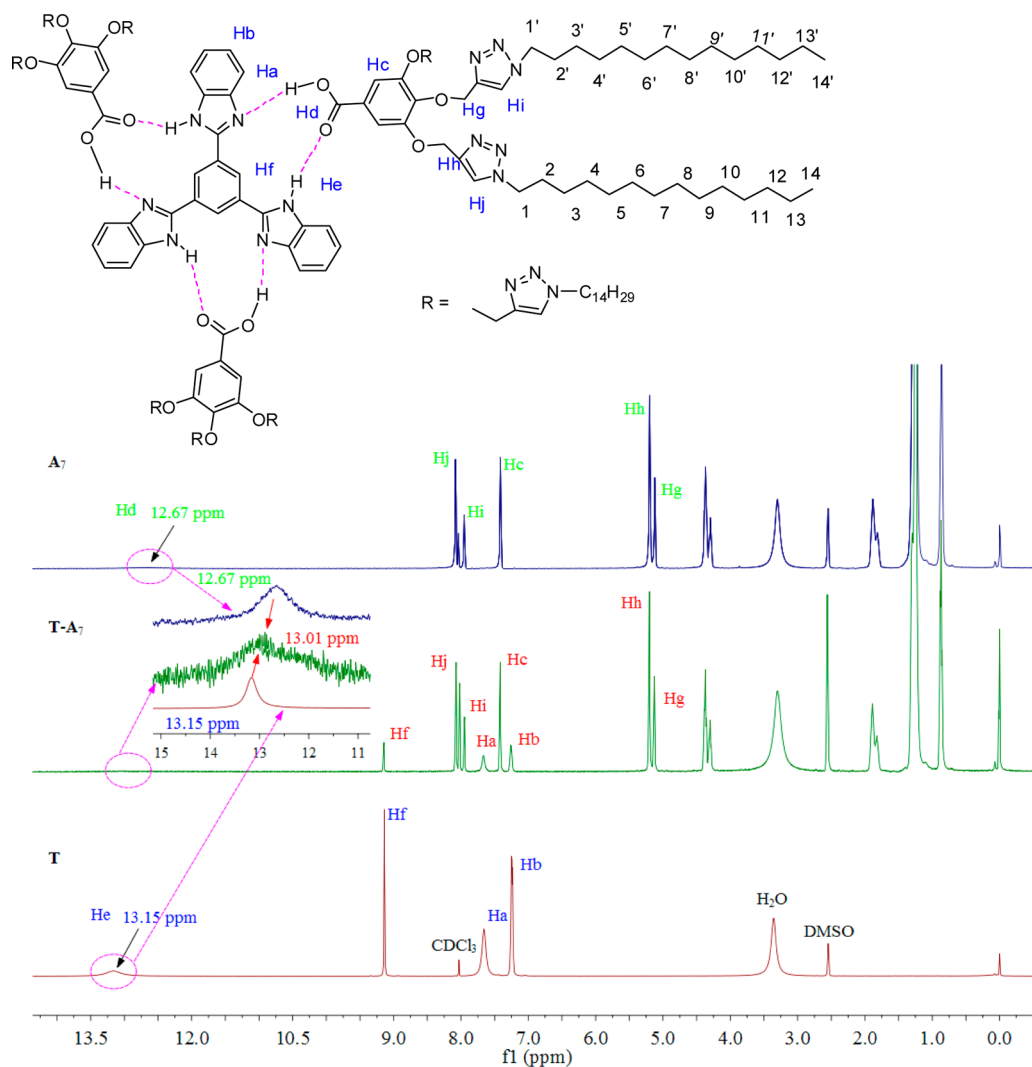


Figure 2. ¹H NMR spectra of **A**₇, the **T-A**₇ complex, and **T** in a CDCl₃/DMSO-*d*₆ mixture at a 1/1 volume ratio.

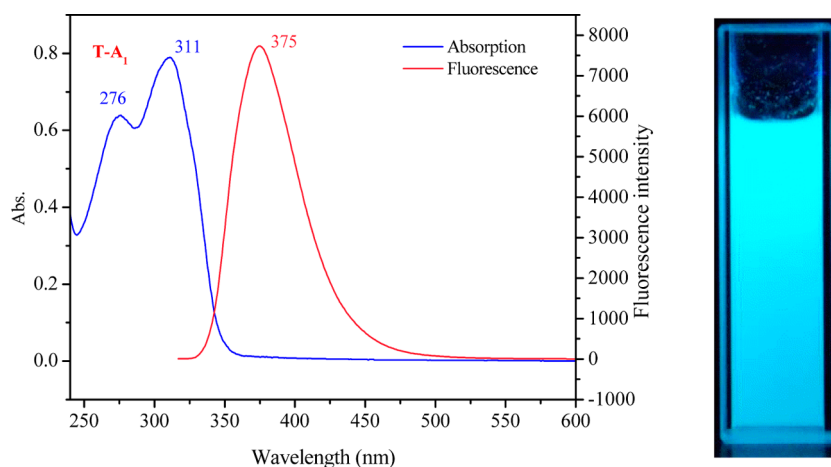


Figure 3. Absorbance and emission spectra of the T-A₁ complex (left) and photograph of the T-A₁ complex in a CH₂Cl₂ solution under 365 nm UV light (right).

corresponding data are different (268, 304, and 367 nm, respectively) because of the difference in the structure of T-A₇ (Scheme 1).

More importantly, in view of the intensity of the band, the T-A₁ complex has absorption and emission stronger than those of the T-A₇ complex (Figure S4 of the Supporting Information), indicating that the T-A₁ complex has photophysical properties relatively better than those of the T-A₇ complex. Furthermore, the CH₂Cl₂ solution (1×10^{-4} mol L⁻¹) of the T-A₁ complex shows very strong blue-green emission under the 365 nm UV light (Figure 3, right). Therefore, the T-A complexes can display a strong fluorescence in solution, which make T-A complexes have a potential application in photoelectric material.^{4–6,15}

For the photoelectric material, thermal stability has an important influence on its performance and lifetime.²⁶ The results of thermogravimetric analysis (Figure S5 of the Supporting Information) are summarized in Table 1.

Table 1. Thermal Stability Data of the T-A Complexes

entry	complex	T_d^a
1	T-A ₁	281.2
2	T-A ₂	285.9
3	T-A ₃	289.7
4	T-A ₄	293.6
5	T-A ₅	244.2
6	T-A ₆	249.9
7	T-A ₇	258.3

^a T_d is the temperature of a 5% mass loss.

Delightedly, in all cases, the T_d , the temperature of a 5% mass loss, is >244 °C, indicating that all T-A complexes have good thermal stability. Upon comparison of entries 5–7 with entries 1–4, it is obvious that the introduction of the triazole moiety is disadvantageous for thermal stability. Even so, their thermal stability still can be comparable to that of some one-component H-bonding liquid crystals.^{27,28}

2.4. Liquid Crystalline Properties. The liquid crystalline (LC) behavior of the final T-A complexes is investigated by polarizing optical microscopy (POM) and differential scanning calorimetry (DSC) (a typical result is shown as Figure 4, and others can be seen in the Supporting Information). Component T or A does not exhibit liquid crystalline properties alone,

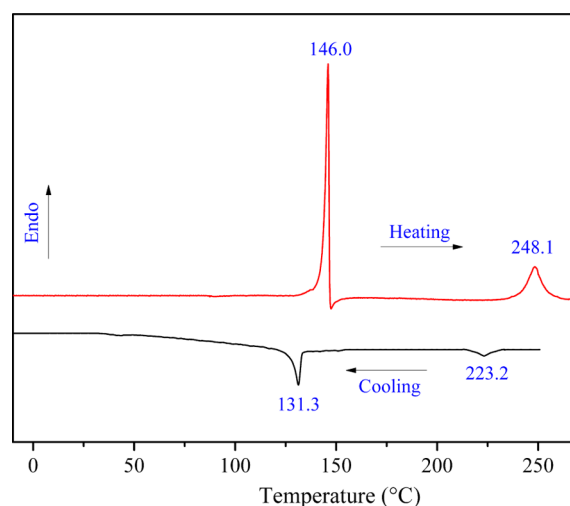


Figure 4. DSC curves of the T-A₇ complex on the first cooling and the second heating runs.

which is similar to the results reported previously,^{15,20} but all T-A complexes can show LC behavior over broad temperature ranges [the largest range is 164.9 °C (Table 2)] with an enantiotropic columnar phase.

Obviously, the temperature range of the LC phase is varied for different components A. For components A₁–A₄, the T-A complexes have a range of >159.6 °C. For A₅–A₇, the range of the LC phase is relatively smaller and just >93.0 °C, which may be related to the introduction of the triazole structure in component A. Recently, there are only two reports about the fluorescent supramolecular columnar liquid crystal based on the H-bonding of two components. Their ranges of the LC phase are 15.0 °C²⁰ and 41.6 °C;¹⁵ both are obviously smaller than the range of our T-A complexes.

The textures observed by POM (Figure 5), on cooling from the isotropic liquid, are consistent with the presence of columnar mesomorphism. Among them, the pseudo focal conic fan-shaped textures as the typical columnar phase textures²⁹ are observed for the T-A complexes for components A₁–A₄ (panels a–d, respectively, in Figure 5). For components A₅–A₇, the T-A complexes have dendritic textures (panels e–g, respectively, in Figure 5), which are also the typical columnar phase textures.³⁰ Thus, there is a difference between these

Table 2. Phase Transition Temperatures (degrees Celsius) and Enthalpies (joules per gram, in parentheses) of T–A Complexes

complex	second heating ^a	first cooling ^a
T–A ₁	Cr-50.4 (64.97)·Colr-208.9 (2.37)·I	I-201.5 (1.99)·Colr-36.6 (65.94)·Cr
T–A ₂	Cr-56.6 (74.04)·Colr-215.8 (2.86)·I	I-208.6 (2.25)·Colr-44.8 (79.13)·Cr
T–A ₃	Cr-75.2 (90.30)·Colr-229.9 (4.77)·I	I-217.8 (3.66)·Colr-58.2 (90.72)·Cr
T–A ₄	Cr-66.4 (79.36)·Colr-220.3 (3.58)·I	I-210.5 (3.29)·Colr-49.6 (79.06)·Cr
T–A ₅	Cr-117.7 (4.86)·Colh-222.5 (0.55)·I	I-207.8 (2.08)·Colh-114.8 (3.56)·Cr
T–A ₆	Cr-124.4 (13.8)·Colh-239.6 (16.06)·I	I-225.9 (18.6)·Colh-114.2 (8.48)·Cr
T–A ₇	Cr-146.0 (18.62)·Colh-248.1 (26.23)·I	I-232.2 (2.58)·Colh-131.3 (10.03)·Cr
HBC-2 ²⁰	–	I-38.1 (7.2)·Colr-23.1 (12.2)·Cr
M-X12E12 ¹⁵	–	I-111.6·Colr-70.0·g

^aAbbreviations: Cr, crystalline; Colr, rectangular columnar mesophase; I, isotropic liquid; g, glassy state that maintains the mesophase organization.

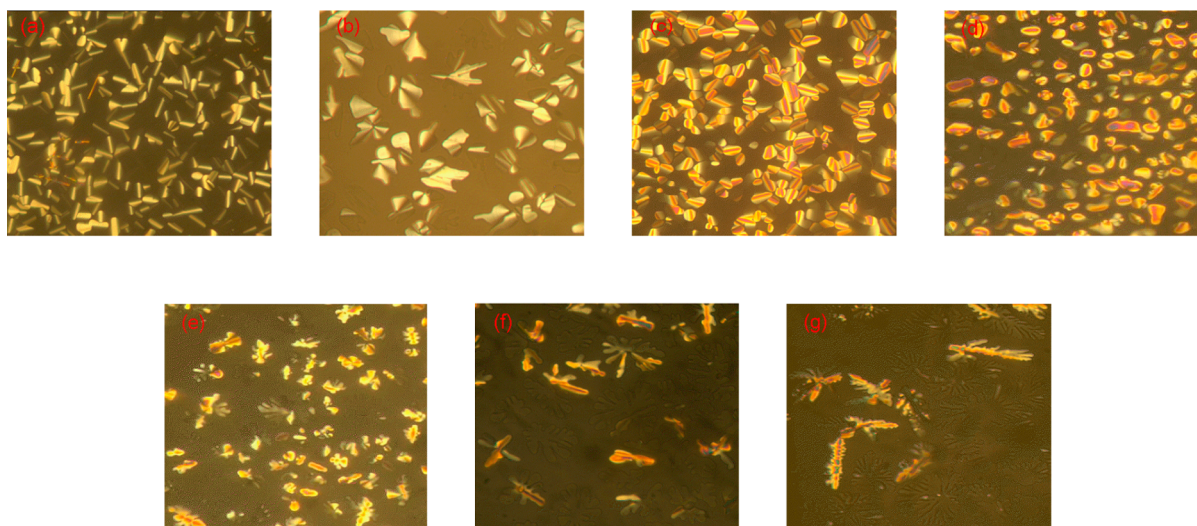


Figure 5. Polarized optical micrographs of T–A complexes: (a) T–A₁ at 128 °C, (b) T–A₂ at 116 °C, (c) T–A₃ at 112 °C, (d) T–A₄ at 123 °C, (e) T–A₅ at 192 °C, (f) T–A₆ at 197 °C, and (g) T–A₇ at 203 °C.

textures, and those of the former four T–A complexes are due to the introduction of the 1,2,3-triazole structure.

The existence of liquid crystalline mesophases of T–A complexes is further confirmed by X-ray diffraction (XRD). Taking T–A₁ and T–A₇ as the representative cases (Figures 6 and 7), their phases are analyzed. The ratio of the Bragg spacing (*d*) at the small angles of the compounds in their mesophases is not 1:1/2:1/3, indicating that their mesophases do not show a

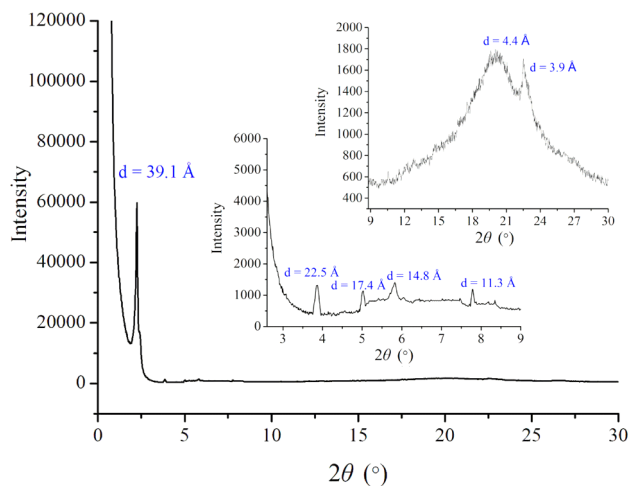


Figure 6. XRD patterns of the T–A₇ complex in the Col phase.

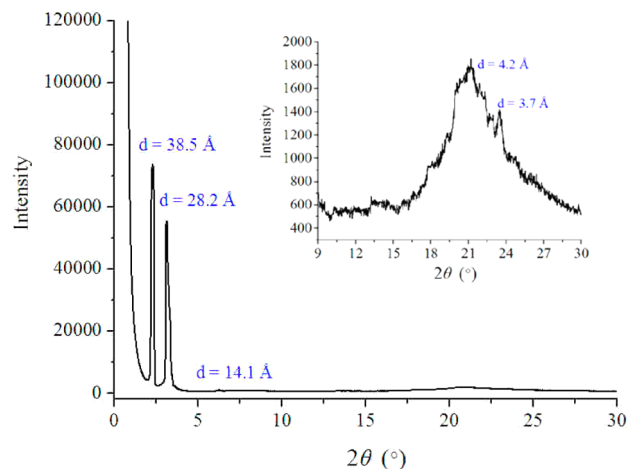


Figure 7. XRD patterns of the T–A₁ complex in the Col phase.

lamellar structure.²⁴ Therefore, in combination with the POM results described above, the phases of the T–A complexes are columnar phases (Col).

For the general discotic liquid crystals, there are two main types of Col phases with *D*_{6h} (hexagonal) and *D*_{2h} (rectangular) symmetries.²⁹ For the T–A₇ complex (Figure 6), it shows one diffraction peak with a *d* spacing of 39.1 Å and four weaker features (22.5, 17.4, 14.8, and 11.3 Å) with a spacing ratio of 1: (1/3)^{1/2}: (1/5)^{1/2}: (1/7)^{1/2}: (1/12)^{1/2} in the small angle region. A

broad halo centered at 4.4 Å and a peak at 3.9 Å are also observed, which are assigned to the spacings between alkyl chains and the central π -systems, respectively. Thus, the XRD data of T-A₇ in conjunction with the textural pattern suggest that the mesophase is indeed the hexagonal columnar phase (Colh).²⁰ Similarly, the liquid crystal phases of T-A₅ and T-A₆ are also Colh (Scheme 1).

The XRD pattern of the T-A₁ complex in its LC phase consists of two strong diffraction peaks with d spacings of 38.5, 28.2, and 14.1 Å in the small angle region, corresponding to the (11), (20), and (40) reflections, respectively. A broad halo centered at 4.2 Å and a peak at 3.7 Å are also observed (Figure 7), which are assigned to the spacings between alkyl chains and the central π -systems, respectively. Thus, in combination with the POM result of the T-A₁ complex, this phase can be assigned to rectangular columnar mesophases (Colr).²⁴ Similarly, the liquid crystal phases of T-A₁, T-A₂, and T-A₃ are also Colr (Scheme 1).

3. CONCLUSION

In summary, a fluorescent core 1,3,5-tri(1*H*-benzo[*d*]imidazol-2-yl)benzene (T) is concisely synthesized and can be successfully designed to form supramolecular T-A complexes through H-bonding with gallic acid derivatives (A). The formation of T-A complexes is characterized by FTIR and ¹H NMR. None of the T and A components present mesomorphism, while all T-A complexes exhibit liquid crystalline profiles. The mesophase properties are studied by POM, DSC, and large and small angle X-ray scattering. Though the introduction of 1,2,3-triazole structure into component A is slightly disadvantageous, all T-A liquid crystal materials show a tendency to exhibit columnar mesomorphism with a broad temperature range (up to 164.9 °C). For the T-A complexes with components A₁–A₄, rectangular columnar mesophases are obtained. While for the T-A complexes with components A₅–A₇, they show the hexagonal columnar mesophases. T-A complexes have strong fluorescence in solution. Furthermore, all T-A complexes display good thermal stability with a high decomposition temperature ($T_d > 240$ °C), and the T_d of some T-A complexes is near 300 °C. Thus, the T-A complexes are characterized as highly organized, strongly fluorescent systems with potential use in photoelectric materials. Also, this will make us investigate the LC materials based on benzimidazoles. In the future, the fluorescent properties of these two-component system supramolecular columnar liquid crystals will be further reported.

4. EXPERIMENTAL SECTION

4.1. General Information. All reagents and solvents were commercially available and used as received. The alkyl azide intermediate was prepared according to the reported procedures.³¹ Melting points were uncorrected. IR spectra were recorded with an FTIR spectrometer. ¹H and ¹³C NMR spectra were recorded with a 400 MHz NMR instrument in CDCl₃ (or DMSO-*d*₆, or their mixed solvent) using TMS as an internal standard. Elemental analysis was performed on an elemental analyzer. Mass spectra (MS) were recorded on a mass spectrometer. UV-vis spectra were measured by an ultraviolet absorption detector. The fluorescence spectra were recorded with a spectrophotometer. The textures of the mesophases were studied with an optical microscope with crossed polarizers. Measurements of the transition temperatures were performed with a thermal analyzer with a heating or cooling rate of 10 °C min⁻¹. Thermogravimetric analysis (TGA) was performed at a heating rate of 10 °C min⁻¹ under a N₂ atmosphere (flow velocity of 20 mL min⁻¹).

X-ray diffraction (XRD) studies were conducted at room temperature with an X-ray diffractometer using Cu K α radiation.¹⁴

4.2. Synthesis of Component Compounds T and A₁–A₇.
4.2.1. 1,3,5-Tri(1*H*-benzo[*d*]imidazol-2-yl)benzene (T). This compound was synthesized as described in the literature:³² yellowish solid; 3.455 g, 81% yield (80%³²); mp >300 °C; UV-vis (DMSO) λ_{max} 316.0 nm; ¹H NMR (400 MHz, DMSO-*d*₆/TMS) δ 7.20–7.52 (m, 6H), 7.62–7.91 (m, 6H), 9.22 (s, 3H), 13.49 (s, 3H); ¹³C NMR (100 MHz, DMSO-*d*₆/TMS) δ 112.2, 119.4, 122.4, 123.4, 125.9, 132.3, 135.8, 144.2, 150.8; ESI-MS calcd for C₂₇H₁₉N₆⁺ ([M + H]⁺) m/z 427.17 (100%), found m/z 427.31 (100%).

4.2.2. 3,4,5-Tris(dodecyloxy)benzoic Acid (A₁). This compound was synthesized as described in the literature:³³ white powder; 1.843 g, 91% yield; mp 55.1–56.0 °C (56 °C³³); ¹H NMR (400 MHz, CDCl₃/TMS) δ 0.88 (t, J = 8.0 Hz, 9H), 1.27–1.35 (m, 48H), 1.44–1.52 (m, 6H), 1.72–1.86 (m, 6H), 4.01–4.06 (m, 6H), 7.33 (s, 2H); IR (film) ν 3070, 2955, 2918, 2850, 1684, 1588, 1508, 1472, 1223, 1125, 867, 770, 720 cm⁻¹; ESI-MS calcd for C₄₃H₇₇O₅⁻ ([M]⁻) m/z 673.58 (100%), found m/z 673.87 (100%).

4.2.3. 3,4,5-Tris(tetradecyloxy)benzoic Acid (A₂). This compound was synthesized as described in the literature:³³ white powder; 2.050 g, 90% yield; mp 42.1–43.5 °C (56%, 43–45 °C³⁴); ¹H NMR (CDCl₃/TMS, 400 MHz) δ 0.88 (t, J = 8.0 Hz, 9H), 1.26–1.35 (m, 60H), 1.44–1.51 (m, 6H), 1.71–1.85 (m, 6H), 4.01–4.06 (m, 6H), 7.32 (s, 2H); ESI-MS calcd for C₄₉H₈₉O₅⁻ ([M]⁻) m/z 757.68 (100%), found m/z 757.98 (100%).

4.2.4. 3,4,5-Tris(hexadecyloxy)benzoic Acid (A₃). This compound was synthesized as described in the literature:³³ white powder; 2.227 g, 88% yield; mp 75.4–77.0 °C (85%, 78 °C²⁴); ¹H NMR (CDCl₃/TMS, 400 MHz) δ 0.91 (t, J = 8.0 Hz, 9H), 1.26–1.32 (m, 72H), 1.47–1.53 (m, 6H), 1.73–1.88 (m, 6H), 4.03–4.09 (m, 6H), 7.35 (s, 2H); ESI-MS calcd for C₅₅H₁₀₁O₅⁻ ([M]⁻) m/z 841.76 (100%), found m/z 841.97 (100%).

4.2.5. 3,4,5-Tris(octadecyloxy)benzoic Acid (A₄). This compound was synthesized as described in the literature:³³ white powder; 2.393 g, 86% yield; mp 47.4–48.9 °C (81%, 47–49 °C³⁵); ¹H NMR (CDCl₃/TMS, 400 MHz) δ 0.88 (t, J = 8.0 Hz, 9H), 1.25–1.30 (m, 84H), 1.44–1.59 (m, 6H), 1.71–1.87 (m, 6H), 4.00–4.05 (m, 6H), 7.31 (s, 2H); ESI-MS calcd for C₆₁H₁₁₃O₅⁻ ([M]⁻) m/z 925.86 (100%), found m/z 925.97 (100%).

4.2.6. Methyl 3,4,5-Tris(prop-2-yn-1-yloxy)benzoate (3). This compound was synthesized as described in the literature:³⁶ white powder; 2.595 g, 87% yield; mp 89.2–90.4 °C (93%, 89.4 °C³⁷); ¹H NMR (CDCl₃/TMS, 400 MHz) δ 2.46 (t, J = 4.0 Hz, 1H), 2.53 (t, J = 4.0 Hz, 2H), 3.91 (s, 3H), 4.80 (d, J = 4.0 Hz, 4H), 4.83 (d, J = 4.0 Hz, 2H), 7.47 (s, 2H); ESI-MS calcd for C₁₇H₁₅O₅⁺ ([M + Na]⁺) m/z 321.07 (100%), found m/z 321.28 (100%).

4.2.7. Methyl 3,4,5-Tris[(1-decyl-1*H*-1,2,3-triazol-4-yl)methoxy]benzoate (5a). A 50 mL flask was charged with intermediate 3 (0.460 g, 2 mmol), *n*-C₁₀H₂₁N₃ 4a (1.466 g, 8 mmol), 10% mmol of Cu, and 5% mmol of CuSO₄ in CH₃CN (5 mL). The reaction mixture was stirred at 25 °C for 48 h. After the reaction had reached completion, the resulting mixture was extracted with ethyl acetate (3 \times 10 mL), and then the organic layer was washed several times with distilled water. After the sample had been dried with anhydrous MgSO₄, the solvent was removed *in vacuo*. The crude product was purified by column chromatography on silica gel with a gradient eluent of mixtures of petroleum ether and ethyl acetate to afford pure sample 5a: white powder; 1.578 g, 93% yield; mp 103.4–104.1 °C; UV-vis (CH₂Cl₂) λ_{max} 264.5 nm; ¹H NMR (CDCl₃/TMS, 400 MHz) δ 0.87 (t, J = 8.0 Hz, 9H), 1.23–1.34 (m, 42H), 1.84–1.87 (m, 2H), 1.89–1.95 (m, 4H), 3.89 (s, 3H), 4.32 (t, J = 8.0 Hz, 2H), 4.36 (t, J = 8.0 Hz, 4H), 5.25 (s, 4H), 5.26 (s, 2H), 7.42 (s, 2H), 7.79 (s, 2H), 7.80 (s, 1H); ¹³C NMR (CDCl₃/TMS, 100 MHz) δ 14.1, 22.63, 26.5, 29.0, 29.2, 29.4, 29.5, 30.2, 30.3, 31.8, 50.3, 50.5, 52.3, 63.3, 66.4, 109.3, 123.1, 123.8, 125.7, 141.6, 143.4, 144.0, 152.0, 166.3; IR (film) ν 3144, 3098, 2959, 2922, 2855, 1727, 1590, 1507, 1462, 1329, 1110, 1054, 837, 761, 721 cm⁻¹; ESI-MS calcd for C₄₇H₇₈N₉O₅⁺ ([M + H]⁺) m/z 848.60 (100%), found m/z 848.77 (100%). Anal. Calcd for

$C_{47}H_{77}N_9O_5$: C, 66.56; H, 9.15; N, 14.86. Found: C, 66.70; H, 9.20; N, 14.72.

4.2.8. Methyl 3,4,5-Tris[(1-dodecyl-1H-1,2,3-triazol-4-yl)methoxy]benzoate (5b). A 50 mL flask was charged with intermediate **3** (0.460 g, 2 mmol), $n\text{-C}_{12}\text{H}_{25}\text{N}_3$ **4b** (1.691 g, 8 mmol), 10% mmol of Cu, and 5% mmol of CuSO_4 in CH_3CN (5 mL). The reaction mixture was stirred at 25 °C for 48 h. After the reaction had reached completion, the resulting mixture was extracted with ethyl acetate (3×10 mL), and then the organic layer was washed several times with distilled water. After the sample had been dried with anhydrous MgSO_4 , the solvent was removed *in vacuo*. The crude product was purified by column chromatography on silica gel with a gradient eluent of mixtures of petroleum ether and ethyl acetate to afford pure sample **5b**: white powder; 1.770 g, 95% yield; mp 107.5–108.3 °C; UV–vis (CH_2Cl_2) λ_{max} 264.0 nm; ^1H NMR (CDCl_3/TMS , 400 MHz) δ 0.88 (t, J = 8.0 Hz, 9H), 1.23–1.34 (m, 54H), 1.84–1.87 (m, 2H), 1.89–1.94 (m, 4H), 3.89 (s, 3H), 4.30 (t, J = 8.0 Hz, 2H), 4.36 (t, J = 8.0 Hz, 4H), 5.25 (s, 4H), 5.26 (s, 2H), 7.42 (s, 2H), 7.79 (s, 2H), 7.80 (s, 1H); ^{13}C NMR (CDCl_3/TMS , 100 MHz) δ 14.1, 22.6, 26.5, 29.0, 29.3, 29.40, 29.5, 29.6, 30.2, 30.3, 31.9, 50.3, 50.5, 52.3, 63.3, 66.4, 109.3, 123.1, 123.8, 125.6, 141.6, 143.6, 144.0, 152.0, 166.3; IR (film) ν 3145, 3096, 2955, 2922, 2852, 1726, 1593, 1500, 1469, 1329, 1113, 1053, 828, 761, 721 cm^{-1} ; ESI-MS calcd for $\text{C}_{53}\text{H}_{90}\text{N}_9\text{O}_5^+$ ($[\text{M} + \text{H}]^+$) m/z 932.71 (100%), found m/z 933.04 (100%). Anal. Calcd for $\text{C}_{53}\text{H}_{90}\text{N}_9\text{O}_5$: C, 68.28; H, 9.62; N, 13.52. Found: C, 68.18; H, 9.76; N, 13.33.

4.2.9. Methyl 3,4,5-Tris[(1-tetradecyl-1H-1,2,3-triazol-4-yl)methoxy]benzoate (5c). A 50 mL flask was charged with intermediate **3** (0.460 g, 2 mmol), $n\text{-C}_{14}\text{H}_{29}\text{N}_3$ **4c** (1.915 g, 8 mmol), 10% mmol of Cu, and 5% mmol of CuSO_4 in CH_3CN (5 mL). The reaction mixture was stirred at 25 °C for 48 h. After the reaction had reached completion, the resulting mixture was extracted with ethyl acetate (3×10 mL), and then the organic layer was washed several times with distilled water. After the sample had been dried with anhydrous MgSO_4 , the solvent was removed *in vacuo*. The crude product was purified by column chromatography on silica gel with a gradient eluent of mixtures of petroleum ether and ethyl acetate to afford pure sample **5c**: white powder; 1.911 g, 94% yield; mp 119.9–120.8 °C; UV–vis (CH_2Cl_2) λ_{max} 265.0 nm; ^1H NMR (CDCl_3/TMS , 400 MHz) δ 0.88 (t, J = 8.0 Hz, 9H), 1.24–1.36 (m, 66H), 1.84–1.87 (m, 2H), 1.89–1.94 (m, 4H), 3.88 (s, 3H), 4.30 (t, J = 8.0 Hz, 2H), 4.36 (t, J = 8.0 Hz, 4H), 5.25 (s, 6H), 7.40 (s, 2H), 7.81 (s, 3H); ^{13}C NMR (CDCl_3/TMS , 100 MHz) δ 14.1, 22.6, 26.4, 26.5, 29.0, 29.3, 29.4, 29.5, 29.6, 30.2, 30.3, 31.9, 50.2, 50.4, 52.2, 63.3, 66.4, 109.2, 123.1, 123.8, 125.6, 141.6, 143.3, 144.0, 152.0, 166.2; IR (film) ν 3151, 3096, 2953, 2918, 2850, 1719, 1593, 1507, 1468, 1328, 1108, 1053, 831, 761, 721 cm^{-1} ; ESI-MS calcd for $\text{C}_{59}\text{H}_{102}\text{N}_9\text{O}_5^+$ ($[\text{M} + \text{H}]^+$) m/z 1016.80 (100%), found m/z 1016.89 (100%). Anal. Calcd for $\text{C}_{59}\text{H}_{101}\text{N}_9\text{O}_5$: C, 69.71; H, 10.02; N, 12.40. Found: C, 69.58; H, 9.85; N, 12.52.

4.2.10. 3,4,5-Tris[(1-decyl-1H-1,2,3-triazol-4-yl)methoxy]benzoic Acid (A₂). A 100 mL flask was charged with intermediate **5a** (0.848 g, 1 mmol) and a solution of NaOH (0.040 g, 1 mmol) in 60 mL of alcohol. After 1 mL of distilled water had been added, the mixture was refluxed for 8 h. Then, the cooled mixture was acidified with dilute HCl to pH 2–3, and the white crude product precipitated. The subsequent recrystallization with anhydrous ethanol gave **A₂**: white powder; 0.726 g, 87% yield; mp 149.2–150.6 °C; UV–vis (CH_2Cl_2) λ_{max} 267.5 nm; ^1H NMR (CDCl_3/TMS , 400 MHz) δ 0.87 (t, J = 8.0 Hz, 9H), 1.23–1.34 (m, 42H), 1.84–1.88 (m, 2H), 1.91–1.95 (m, 4H), 4.31 (t, J = 8.0 Hz, 2H), 4.36 (t, J = 8.0 Hz, 4H), 5.27 (s, 6H), 6.81 (b, 1H), 7.49 (s, 2H), 7.82 (s, 1H), 7.83 (s, 2H); ^{13}C NMR (CDCl_3/TMS , 100 MHz) δ 14.1, 22.6, 26.5, 29.0, 29.2, 29.4, 29.5, 30.2, 30.3, 31.8, 50.4, 50.6, 63.0, 66.3, 109.7, 123.3, 123.9, 126.0, 141.8, 143.6, 144.0, 144.1, 151.9, 169.0; IR (film) ν 3456, 3141, 3090, 2959, 2922, 2853, 1700, 1593, 1507, 1464, 1328, 1123, 1051, 832, 768, 723 cm^{-1} ; ESI-MS calcd for $\text{C}_{46}\text{H}_{76}\text{N}_9\text{O}_5^+$ ($[\text{M} + \text{H}]^+$) m/z 834.60 (100%), found m/z 834.76 (100%). Anal. Calcd for $\text{C}_{46}\text{H}_{75}\text{N}_9\text{O}_5$: C, 66.23; H, 9.06; N, 15.11. Found: C, 66.39; H, 9.00; N, 15.28.

4.2.11. 3,4,5-Tris[(1-dodecyl-1H-1,2,3-triazol-4-yl)methoxy]benzoic Acid (A₆). A 100 mL flask was charged with intermediate

5b (0.932 g, 1 mmol) and a solution of NaOH (0.040 g, 1 mmol) in 60 mL of alcohol. After 1 mL of distilled water had been added, the mixture was refluxed for 8 h. Then, the cooled mixture was acidified with dilute HCl to pH 2–3, and the white crude product precipitated. The subsequent recrystallization with anhydrous ethanol gave **A₆**: white powder; 0.817 g, 89% yield; mp 152.4–153.6 °C; UV–vis (CH_2Cl_2) λ_{max} 267.0 nm; ^1H NMR (CDCl_3/TMS , 400 MHz) δ 0.87 (t, J = 8.0 Hz, 9H), 1.22–1.35 (m, 54H), 1.83–1.88 (m, 2H), 1.91–1.97 (m, 4H), 4.31 (t, J = 8.0 Hz, 2H), 4.36 (t, J = 8.0 Hz, 4H), 5.27 (s, 6H), 6.79 (b, 1H), 7.49 (s, 2H), 7.82 (s, 1H), 7.83 (s, 2H); ^{13}C NMR (CDCl_3/TMS , 100 MHz) δ 14.1, 22.6, 26.5, 29.0, 29.2, 29.4, 29.5, 30.2, 30.3, 31.8, 50.4, 50.6, 66.0, 66.3, 109.7, 123.3, 123.9, 126.0, 141.8, 143.4, 144.0, 144.1, 151.9, 169.0; IR (film) ν 3442, 3146, 3093, 2957, 2922, 2855, 1695, 1588, 1504, 1464, 1321, 1112, 1049, 825, 797, 731 cm^{-1} ; ESI-MS calcd for $\text{C}_{52}\text{H}_{88}\text{N}_9\text{O}_5^+$ ($[\text{M} + \text{H}]^+$) m/z 918.69 (100%), found m/z 918.79 (100%). Anal. Calcd for $\text{C}_{52}\text{H}_{87}\text{N}_9\text{O}_5$: C, 68.01; H, 9.55; N, 13.73. Found: C, 68.19; H, 9.36; N, 13.60.

4.2.12. 3,4,5-Tris[(1-tetradecyl-1H-1,2,3-triazol-4-yl)methoxy]benzoic Acid (A₇). A 100 mL flask was charged with intermediate **5c** (1.016 g, 1 mmol) and a solution of NaOH (0.040 g, 1 mmol) in 60 mL of alcohol. After 1 mL of distilled water had been added, the mixture was refluxed for 8 h. Then, the cooled mixture was acidified with dilute HCl to pH 2–3, and the white crude product precipitated. The subsequent recrystallization with anhydrous ethanol gave **A₇**: white powder; 0.902 g, 90% yield; mp 154.2–155.8 °C; UV–vis (CH_2Cl_2) λ_{max} 266.5 nm; ^1H NMR (CDCl_3/TMS , 400 MHz) δ 0.87 (t, J = 8.0 Hz, 9H), 1.22–1.35 (m, 66H), 1.84–1.96 (m, 6H), 4.28–4.40 (m, 6H), 5.28 (s, 6H), 6.41 (b, 1H), 7.50 (s, 2H), 7.82 (s, 3H); ^{13}C NMR (CDCl_3/TMS , 100 MHz) δ 14.1, 22.7, 26.5, 26.6, 29.0, 29.1, 29.3, 29.4, 29.5, 29.6, 30.3, 30.4, 31.9, 50.5, 50.7, 63.2, 66.5, 109.9, 123.4, 124.1, 125.7, 142.0, 143.4, 144.1, 152.0, 169.1; IR (film) ν 3451, 3140, 3089, 2955, 2919, 2848, 1700, 1593, 1507, 1466, 1320, 1119, 1054, 842, 764, 724 cm^{-1} ; ESI-MS calcd for $\text{C}_{58}\text{H}_{100}\text{N}_9\text{O}_5^+$ ($[\text{M} + \text{H}]^+$) m/z 1002.78 (100%), found m/z 1002.87 (100%). Anal. Calcd for $\text{C}_{58}\text{H}_{99}\text{N}_9\text{O}_5$: C, 69.49; H, 9.95; N, 12.58. Found: C, 69.36; H, 9.86; N, 12.70.

4.3. Preparation of the T–A Complexes. Taking complex **T–A₁** as an example, we prepared the T–A complexes as follows. Component **T** (0.0426 g, 0.1 mmol) was dissolved in 60 mL of methanol by refluxing for 1 h, and then the solution of component **A₁** (0.2025 g, 0.3 mmol) in 10 mL of CHCl_3 was added. The mixture was refluxed for 4 h. After the solvent had evaporated *in vacuo*, drying *in vacuo* gave complex **T–A₁** in a yield of 100%. According to a similar method, the other six T–A complexes were also quantitatively obtained.

Some typical characterization data of T–A complexes. For complex **T–A₁**: ^1H NMR (CDCl_3/TMS , 400 MHz) δ 0.85–0.91 (m, 27H), 1.20–1.38 (m, 144H), 1.45–1.55 (m, 18H), 1.74–1.88 (m, 18H), 3.93–4.10 (m, 18H), 7.20–7.22 (m, 6H), 7.40 (s, 6H), 7.60–7.63 (m, 6H), 9.53 (s, 3H). For complex **T–A₇**: ^1H NMR ($\text{CDCl}_3/\text{DMSO}-d_6/\text{TMS}$, 400 MHz) δ 0.85–0.89 (m, 27H), 1.24–1.27 (m, 180H), 1.29–1.32 (m, 18H), 1.80–1.85 (m, 6H), 1.86–1.91 (m, 12H), 4.30 (t, J = 8.0 Hz, 6H), 4.37 (t, J = 8.0 Hz, 12H), 5.13 (s, 6H), 5.20 (s, 12H), 7.14–7.34 (m, 6H), 7.41–7.44 (m, 6H), 7.56–7.77 (m, 6H), 7.94–7.96 (m, 3H), 8.06–8.09 (m, 6H), 9.14 (s, 3H), 13.01 (b, 6H).

Before being used in further test experiments, all T–A complexes were heated to the isotropic state and then slowly cooled to room temperature to make the mesophase completely formed according to the literature.^{13,15,18,20}

■ ASSOCIATED CONTENT

● Supporting Information

Some detailed discussions and explanations with supplied figures and tables; ^1H and ^{13}C NMR and mass spectra of compounds **T**, **A₁–A₄**, **3**, **5a–5c**, and **A₅–A₇**; and ^1H NMR spectra of typical T–A complexes. This material is available free of charge via the Internet at <http://pubs.acs.org>.

AUTHOR INFORMATION

Corresponding Authors

*E-mail: cescsx@mail.sysu.edu.cn.

*E-mail: wangzy@scnu.edu.cn. Telephone: 8620-39310258.

Author Contributions

[†]J.-F. Xiong and S.-H. Luo contributed equally to this work.

Notes

The authors declare no competing financial interest.

ACKNOWLEDGMENTS

We are grateful to the National Natural Science Foundation of China (20772035), the 3rd Talents Special Funds of Guangdong Higher Education (Guangdong-Finance-Education [2011]431), and the Natural Science Foundation of Guangdong Province (S2011010001556) for financial support.

REFERENCES

- Broer, D. J.; Bastiaansen, C. M. W.; Debije, M. G.; Schenning, A. P. H. J. *Angew. Chem., Int. Ed.* **2012**, *51*, 7102–7109.
- Wong, J. P.-W.; Whitwood, A. C.; Bruce, D. W. *Chem.—Eur. J.* **2012**, *18*, 16073–16089.
- Reddy, M. K.; Reddy, K. S.; Narasimhaswamy, T.; Das, B. B.; Lobo, N. P.; Ramanathan, K. V. *New J. Chem.* **2013**, *37*, 3195–3206.
- Yasuda, T.; Shimizu, T.; Liu, F.; Ungar, G.; Kato, T. *J. Am. Chem. Soc.* **2011**, *133*, 13437–13444.
- Kelber, J.; Achard, M.-F.; Durola, F.; Bock, H. *Angew. Chem., Int. Ed.* **2012**, *51*, S200–S203.
- Araoka, F.; Masuko, S.; Kogure, A.; Miyajima, D.; Aida, T.; Takezoe, H. *Adv. Mater.* **2013**, *25*, 4014–4017.
- Demenev, A.; Eichhorn, S. H.; Taerum, T.; Perepichka, D. F.; Patwardhan, S.; Grozema, F. C.; Siebbeles, L. D. A.; Klenkler, R. *Chem. Mater.* **2010**, *22*, 1420–1428.
- Miyajima, D.; Araoka, F.; Takezoe, H.; Kim, J.; Kato, K.; Takata, M.; Aida, T. *J. Am. Chem. Soc.* **2010**, *132*, 8530–8531.
- Fitie, C. F. C.; Roelofs, W. S. C.; Magusin, P. C. M. M.; Wübbenhorst, M.; Kemerink, M.; Sijbesma, R. P. *J. Phys. Chem. B* **2012**, *116*, 3928–3937.
- Moyano, S.; Barbera, J.; Diosdado, B. E.; Serrano, J. L.; Elduque, A.; Gimenez, R. *J. Mater. Chem. C* **2013**, *1*, 3119–3128.
- Mes, T.; Cantekin, S.; Balkenende, D. W. R.; Frissen, M. M. M.; Gillissen, M. A. J.; de Waal, B. F. M.; Voets, I. K.; Meijer, E. W.; Palmans, A. R. A. *Chem.—Eur. J.* **2013**, *19*, 8642–8649.
- Elgueta, E. Y.; Parra, M. L.; Díaz, E. W.; Barberá, J. *Liq. Cryst.* **2014**, *41*, 861–871.
- Barbera, J.; Puig, L.; Romero, P.; Serrano, J. L.; Sierra, T. *J. Am. Chem. Soc.* **2006**, *128*, 4487–4492.
- Vera, F.; Barberá, J.; Romero, P.; Serrano, J. L.; Ros, M. B.; Sierra, T. *Angew. Chem., Int. Ed.* **2010**, *49*, 4910–4914.
- Vieira, A. A.; Gallardo, H.; Barberá, J.; Romero, P.; Serrano, J. L.; Sierra, T. *J. Mater. Chem.* **2011**, *21*, S916–S922.
- Moreno, J. R. A.; González, J. J. L.; Ureña, F. P.; Vera, F.; Ros, M. B.; Sierra, T. *J. Phys. Chem. B* **2012**, *116*, 5090–5096.
- Piermattei, A.; Giesbers, M.; Marcelis, A. T. M.; Mendes, E.; Picken, S. J.; Crego-Calama, M.; Reinhoudt, D. N. *Angew. Chem., Int. Ed.* **2006**, *45*, 7543–7546.
- Xu, M.; Chen, L.-Q.; Zhou, Y.-F.; Yi, T.; Li, F.-Y.; Huang, C.-H. *J. Colloid Interface Sci.* **2008**, *326*, 496–502.
- Kohlmeier, A.; Janietz, D. *Chem.—Eur. J.* **2010**, *16*, 10453–10461.
- Ryu, M.-H.; Choi, J.-W.; Kim, H.-J.; Park, N.; Cho, B.-K. *Angew. Chem., Int. Ed.* **2011**, *50*, S737–S740.
- Yagai, S.; Usui, M.; Seki, T.; Murayama, H.; Kikkawa, Y.; Uemura, S.; Karatsu, T.; Kitamura, A.; Asano, A.; Seki, S. *J. Am. Chem. Soc.* **2012**, *134*, 7983–7994.
- Ishihara, S.; Furuki, Y.; Hill, J. P.; Ariga, K.; Takeoka, S. *J. Nanosci. Nanotechnol.* **2014**, *14*, S130–S137.
- Bhalla, V.; Gupta, A.; Kumar, M.; Shankar Rao, D. S.; Prasad, S. K. *ACS Appl. Mater. Interfaces* **2013**, *5*, 672–679.
- Li, J. Z.; Tang, T.; Li, F.; Li, M. *Dyes Pigm.* **2008**, *77*, 395–401.
- Ye, Q.; Chang, J.-J.; Shao, J.-J.; Chi, C.-Y. *J. Mater. Chem.* **2012**, *22*, 13180–13186.
- Tao, Y.-T.; Yang, C.-L.; Qin, J.-G. *Chem. Soc. Rev.* **2011**, *40*, 2943–2970.
- Wiggins, K. M.; Kerr, R. L.; Chen, Z.; Bielawski, C. W. *J. Mater. Chem.* **2010**, *20*, S709–S714.
- Ji, S.-P.; Tang, M.; He, L.; Tao, G.-H. *Chem.—Eur. J.* **2013**, *19*, 4452–4461.
- Yelamagad, C. V.; Achalkumar, A. S.; Rao, D. S. S.; Prasad, S. K. *J. Org. Chem.* **2007**, *72*, 8308–8318.
- Paquette, J. A.; Yardley, C. J.; Psutka, K. M.; Cochran, M. A.; Calderon, O.; Williams, V. E.; Maly, K. E. *Chem. Commun.* **2012**, *48*, 8210–8212.
- Tan, Y.-H.; Li, J.-X.; Xue, F.-L.; Qi, J.; Wang, Z.-Y. *Tetrahedron* **2012**, *68*, 2827–2843.
- Chandrashekar, N.; Thomas, B.; Gayathri, V.; Ramanathan, K. V.; Gowda, N. M. N. *Magn. Reson. Chem.* **2008**, *46*, 769–774.
- Borisch, K.; Diele, S.; Göring, P.; Kresse, H.; Tschierske, C. *J. Mater. Chem.* **1998**, *8*, 529–543.
- Hunter, C. A.; Jones, P. S.; Tiger, P.; Tomas, S. *Chem.—Eur. J.* **2002**, *8*, S435–S446.
- Iqbal, P.; Mayandithevar, M.; Childs, L. J.; Hannon, M. J.; Spencer, N.; Ashton, P. R.; Preece, J. A. *Materials* **2009**, *2*, 146–168.
- Zhang, S. Y.; Zhao, Y. *Bioconjugate Chem.* **2011**, *22*, S23–S28.
- Camponovo, J.; Ruiz, J.; Cloutet, E.; Astruc, D. *Chem.—Eur. J.* **2009**, *15*, 2990–3002.